Global Analysis of Altered Gene Expressions during the Process of Esophageal Squamous Cell Carcinogenesis in the Rat: A Study Combined with a Laser Microdissection and a cDNA Microarray

Koujiro Nishida,[1] Shinji Mine,[1,2] Tohru Utsunomiya,[1] Hiroshi Inoue,[1] Masahiro Okamoto,[1] Harushi Udagawa,[2] Taizo Hanai,[3] and Masaki Mori[1]

[1]Department of Surgery Medical Institute of Bioregulation, Kyushu University, Tsurumihara, Beppu, Japan; [2]Department of Digestive Surgery, Toranomon Hospital and Okinaka Memorial Institute for Medical Research, Toranomon, Minato-ku, Tokyo, Japan; and [3]Laboratory for Bioinformatics, Graduate School of Systems Life Sciences, Kyushu University, Hakozaki, Higashi-ku, Fukuoka, Japan

Abstract

The genetic alterations that occur during esophageal tumorigenesis have yet to be determined. We previously established a Wister rat carcinogenesis model of esophageal squamous cell carcinoma. To understand more about the molecular mechanisms during carcinogenesis, we produced esophageal neoplastic lesions by administering *N*-amyl-*N*-methylnitrosamine and 12-*O*-tetradecanoylphorbol-13-acetate to rats. We used laser microdissection to specifically isolate the cells from the normal epithelium, papilloma, dysplasia, and invasive carcinoma. Using a cDNA microarray representing 14,815 clones, we then analyzed the gene expression profiles for each esophageal lesion. The number of differentially expressed genes compared with the normal control dramatically increased in a step-by-step fashion from normal epithelium (1,151 ± 119 genes) to papilloma (1,899 ± 543 genes), dysplasia (1,991 ± 193 genes), and invasive carcinoma (2,756 ± 87 genes). A hierarchical clustering analysis showed that the three stages of normal epithelium, dysplasia (papilloma), and invasive carcinoma could be clearly classified, whereas the gene expression patterns of papilloma and dysplasia were indistinguishable. Using the Fisher criterion, we also identified 50 genes whose expression level had either significantly increased or decreased in a step-by-step manner from the normal epithelium to dysplasia and then finally to invasive carcinoma. Many of these genes were not previously known to be associated with esophageal carcinogenesis. The present findings in our rat model thus seem to provide us with a better understanding of the molecular alterations that occur during esophageal carcinogenesis and hopefully will also help lead to the development of novel diagnostic and therapeutic targets. (Cancer Res 2005; 65(2): 401-9)

Introduction

We previously established a rat carcinogenesis model of esophageal squamous cell carcinoma (ESCC) by administering *N*-amyl-*N*-methylnitrosamine (AMN) as an initiator, and 12-*O*-tetradecanoylphorbol-13-acetate (TPA, a phorbol diester) as a promoter. In this model, papilloma, dysplasia, and invasive carcinoma were successfully developed by the combined administration of AMN and TPA. Our findings suggest this model to be useful to both investigate and characterize the malignant lesions occurring in the esophagus (1). Since publishing our earlier findings, our knowledge of molecular pathogenesis during cancer development has dramatically improved. For example, the process of colon carcinogenesis has been well documented as an adenoma-carcinoma sequence. In this theoretical model, multistep genetic alterations were clarified, such as the deletion and mutation of the APC, the mutation of the K-*ras*, and abnormalities in the 17th and 18th chromosomes (2, 3). Regarding esophageal carcinogenesis, an increased expression of cyclin D1 was observed not only in esophageal carcinoma but also in precancerous dysplastic lesions (4, 5). An accumulation of p53 protein was also found in the cell nuclei of precancerous and cancerous lesions of the esophagus (6). Although such genetic alterations are possibly early events of esophageal carcinogenesis, there is still a need to clarify these processes at a molecular level. The recent development of large-scale gene expression profiling by DNA microarrays now allows for the concurrent analysis of thousands of genes, and the molecular pathways possibly involved in human ESCC tissues (7–10) and esophageal cancer cell lines (11–13) have also been reported. Most of the former microarray studies compared the gene expression profiles between ESCC tissues and matched normal tissues, however, few studies have investigated the expressional changes during multistep carcinogenesis (7). Furthermore, all of these data derived from bulk tumor tissues might not adequately reflect the cell-type specific expression profiles, because ESCC contain various types of cells, such as mesenchymal cells and inflammatory cells. Indeed, the proportions of neoplastic cells in such tissue samples are quite different from one case to another. On the other hand, several animal studies have shown the molecular changes during tumorigenesis by a technique of DNA microarray (14–18). Again, these studies examined the gene expression patterns of bulk tumor tissues. Taking all of these issues into account, we reproduced our rat carcinogenesis model and prepared purified proportions of the cells by means of laser microdissection (LMD). To the best of our knowledge, this is the first study to identify the global gene expression profiles during the process of multistep carcinogenesis by integrating the technologies combined with LMD and cDNA microrarray. The present findings in our rat model would greatly help us to understand the molecular alterations during esophageal carcinogenesis as well as also help us to identify novel diagnostic and therapeutic targets.

Materials and Methods

Animals and Chemicals. Wistar rats, 4-week-old males, obtained from Nihon Seibutsu Zairyo Center, Tokyo, Japan, were allowed free access to a

Requests for reprints: Masaki Mori, Department of Molecular and Surgical Oncology, Medical Institute of Bioregulation, Kyushu University, Tsurumihara 4546, Beppu, 874-0838, Japan. Phone: 81-977-27-1650; Fax: 81-977-27-1651; E-mail: mmori@tsurumi.beppu.kyushu-u.ac.jp.

standard laboratory chow diet (Oriental Koubo Co., Tokyo, Japan) and water for 7 days before commencing the experiments. All the experimental animals used in this study received humane care according to the guidelines outlined in the Guide for the Care and Use of Laboratory Animals by the National Academy of Science (NIH publication no. 86-23, revised 1985). As described previously (1), AMN was dissolved in tap water at a final concentration of 0.003% and was given to these rats *ad libitum*. TPA was dissolved in pure acetone to a concentration of 0.1 mg/mL and was added to the drinking water to reach a final concentration of 0.1 g/mL. This diluted solution was freshly prepared every 2 days.

Experimental Groups. The 24 rats were divided into four groups with the following treatment regimens: group A, AMN for 4 weeks; group B, AMN for 4 weeks followed by TPA for 8 weeks; group C, AMN for 12 weeks followed by TPA for 4 weeks; group D, untreated controls received neither AMN nor TPA (Table 1).

Tissue Sampling. All rats were observed for 20 weeks from the beginning of treatment and were sacrificed at the end of the experiment. The esophagus from every rat was cut out and the tissue blocks from the normal esophageal epithelium, papilloma, dysplasia, and carcinoma were obtained. Each block was cut into two pieces, with one half being used for the pathologic diagnosis, and the other half being used for the molecular analysis. The latter halves were immediately embedded in a Tissue Tek OCT compound medium (Sakura, Tokyo, Japan) and kept frozen at −80°C until they were microdissected.

Histologic Examination. The pathologic diagnosis was done with H&E staining. Papilloma was characterized by exophytic tumors of squamous cell type with hyperkeratinization. The basal layer of the papilloma was well preserved, and the cellular and nuclear atypism was slight (19, 20). Dysplasia included amorphous cells extending from the basal cell layer, except for a thin superficial layer. If all layers of the epithelium showed dysplastic change, the lesions were defined as carcinoma *in situ*. When invasion was beneath the basement membrane and severe cellular atypism was present, the lesion was described as invasive carcinoma (21). Because it was difficult to clearly distinguish carcinoma *in situ* from severe dysplasia, we decided to exclude carcinoma *in situ* from this study.

Laser Microdissection. For LMD, the Application Solutions Laser Microdissection System (Leica Microsystems, Wetzlar, Germany) was used. Serial 8-μm-thick sections were prepared with a cryostat and were mounted onto a foil-coated glass slide, 90 FOIL-SL25 (Leica Microsystems). The sections were then fixed in 100% ethanol for 3 minutes and stained with H&E staining protocol to maintain the morphologic quality required for accurate microdissection. After careful drying, the sections were laser microdissected according to the manufacturer's instructions (Leica Microsystems).

RNA Extraction, T7-Based RNA Amplification, and Quality Check of Amplified RNAs. Total RNAs were extracted from each sample of laser microdissected cells into 350 μL of buffer RLT (Qiagen, Hilden, Germany) added β-mercaptoethanol to a concentration of 1%. Next, total RNAs were purified with the RNeasy Mini Kit (Qiagen) according to the manufacturer's protocol. All of the total RNAs were subjected to two rounds of T7-based RNA amplification as described previously (22). In brief, whole total RNA was reverse-transcribed by using oligo-dT T7 primer containing the T7 RNA polymerase binding site (5′-AAAC-GACGGCCAGTGAATTGTAATACGACTCACTATAGGCGCT15-3′; refs. 23, 24). Next, second strand cDNA synthesis was done with RNase H, *Escherichia coli* DNA polymerase I and T4 DNA polymerase (TaKaRa Shuzo, Shiga, Japan). The cDNA was then purified and transcribed with MEGA script T7 Transcription Kits (Ambion, Inc., Austin, TX). The purity and concentration of amplified RNA (aRNA) were determined by Agilent 2100 bioanalyzer (Agilent Technologies, Palo Alto, CA).

cDNA Microarray (Labeling, Hybridization, and Scanning). We used the Rat cDNA Microarray (Agilent Technologies) which contains 14,815 clones with 7,575 annotated genes, 5,769 expressed sequence tag clones, and 1,471 other unnamed clones. A list of genes on this cDNA microarray is available at http://www.agilent.com/chem/genelists. Five hundred nanogram aliquots of each aRNA from the 12 esophageal tissue samples (three samples from each of normal esophageal epithelium, papilloma, dysplasia, and invasive carcinoma) were labeled with Cyanine 5-dUTP (Perkin-Elmer/NEN, Boston, MA), whereas a 500-ng aliquot of aRNA from a mixture of three normal esophageal epithelium were labeled with Cyanine 3-dUTP as control. The labeled probes were then hybridized with the rat cDNA microarray in hybridization buffer (Agilent Technologies) for 17 hours at 65°C. After hybridization, the slides were washed in 0.5× SSC/0.01% SDS for 5 minutes at room temperature and 0.06× SSC for 2 minutes at room temperature (25). The Cy3 and Cy5 fluorescent intensities for each spot were determined by an Agilent DNA Microarray Scanner and then were analyzed by G2566AA Feature Extraction Software vA.6.1.1 (Agilent Technologies), which used the LOWESS (locally weighed linear regression curve fit) normalization method (26).

cDNA Microarray Data Analysis. After subtracting the local and global background signals, the expression values were calculated as the log ratio of the dye-normalized red (Cy 5) and green (Cy 3) channel signals. The data flagged as being of poor quality according to the Agilent data extraction software were removed from the analysis. All data calculated by data extraction software were imported to the Rosetta Luminator system v2.0. (Rosetta Biosoftware, Kirkland, WA). All the intensity data were plotted as a log ratio. Next, a hierarchical clustering analysis was done using the Rosetta Luminator system. The gene expression profiles of three stages, including normal epithelium, dysplasia, and invasive carcinoma were further analyzed and compared. To compute the Fisher criterion, three stages were divided into two patterns of two groups as follows: Pattern 1, a group of normal epithelium and dysplasia versus a group of invasive carcinoma; Pattern 2, a group of normal epithelium versus a group of dysplasia and invasive carcinoma. First, we identified the top 500 genes from each pattern. We then selected the genes common to the top 500 genes (302 up-regulated and 198 down-regulated) in Pattern 1 and those (226 up-regulated and 274 down-regulated) in Pattern 2. The original data will be available at URL of supplemental web site at http://www.mib-beppu.kyushu-u.ac.jp/MIB_res/clin_surg/MA/MA_data.html.

Real-time reverse transcription-PCR Assay. The real-time reverse transcription-PCR (RT-PCR) assay was done using the same aRNA samples

Table 1. Development of papilloma, dysplasia, and invasive carcinoma in the rat esophagus

Group	Treatment	No. rats	Lesion incidence (%)		
			Papilloma	Dysplasia	Carcinoma
A	AMN, 4 wk	6	33	33	0
B	AMN, 4 wk → TPA, 8 wk	6	33	50	17
C	AMN, 12 wk → TPA, 4 wk	6	67	33	83
D	No treatment, control	6	0	0	0

that had served for the microarray analysis. The following primers were used to amplify the genes of interest: Rat matrix metalloproteinase 2 (*Mmp2;* F-TCAAGTTCCCCGGCGATGTC and R-TTGCGGGGAAA-GAAGTTGTAGT), Rat cathepsin H (*Ctsh;* F-GTGCCCAGAACTTCAACAATCAT and R-AACGCGACGGCCTTTTCTG), Rat serine protease (*C1s;* F-GGCCA-GAGGTCCAGCAAGAG and R-GGGGGCAGGAGCAGAAGTATC), Rat DRAL (*Fhl2;* F-GAAGCAGCTATCTGGGCAAC and R-TGGCGTTCCTCAAAAGAGAT). Rat aldehyde dehydrogenase (*Aldh1a1;* F-GGGCAGCGATCTCCTCTCACAT and R-CAAGTCGGCATCTGCAAACACAA). Rat cytochrome *P*4502F4 (*Cyp2f1;* F-GGGGCCCAGGCGTGTGATT and R-TCCGCTCCTCGATGCTTCTTTT). Rat *β-actin* (F-CCTAAGGCCAACCGTGAAAAGATG and R-GTCCCGGCCAGC-CAGGTCCAG) was used as an internal standard.

Statistical Methods. The data were expressed as the means ± SD. We used Student's *t* test and Fisher's exact test to assess differences. These data were analyzed with StatView for Windows version 5.01 (SAS Institute, Inc., Cary, NC), and the findings were considered significant when the $P < 0.05$.

Results

Macroscopic and Histologic Findings during Rat Esophageal Carcinogenesis. The macroscopic findings of each lesion are shown in Fig. 1. A histologic examination confirmed each lesion including papilloma, dysplasia, and invasive carcinoma in our rat model (Fig. 1). The incidences of each lesion among the four groups are summarized in Table 1. Papilloma and dysplasia were observed in groups A, B, and C treated with AMN. Group C exhibited a higher incidence of invasive carcinoma than the other groups. There was no detectable papilloma, dysplasia, or carcinoma in group D treated with neither AMN nor TPA. The histologic features of all esophageal carcinomas were squamous cell origin.

T7-Based RNA Amplification and Quality Check of Amplified RNAs. One of the most important steps in gene expression workflow was the quality assessment of RNA samples to ensure the success of gene expression analysis. The purity and concentration of aRNAs were carefully determined using an Agilent 2100 bioanalyzer (Agilent Technologies). Representative electropherograms of successful RNA amplification from each lesion are shown in Fig. 2. High-quality aRNA run on a bioanalyzer typically has the shape of a hump peak, which means no contamination of rRNA. Two rounds of T7-based RNA amplification yielded 5 to 40 μg of aRNA from each sample, and they were sufficient to perform cDNA microarray (27, 28). We successfully obtained high-quality aRNAs, of which quality were verified with the bioanalyzer, from 12 esophageal tissue samples (three samples each of normal epithelium, papilloma, dysplasia, and invasive carcinoma). All of them were employed for the following cDNA microarray analysis.

cDNA Microarray Data Analysis. All intensity data were plotted as a log ratio with the Rosetta Luminator system (Rosetta Biosoftware). The number of differentially expressed genes remarkably increased during the process of esophageal carcinogenesis (Fig. 3). In the normal epithelium, 1,151 ± 119 clones were determined as differentially expressed genes in comparison with the normal control (mixture of three normal epithelium), indicating a high correlation coefficient ($R = 0.93 \pm 0.03$). In contrast, 1,899 ± 543 clones in papilloma ($R = 0.87 \pm 0.05$) and 1,991 ± 193 clones in dysplasia ($R = 0.87 \pm 0.03$) were determined as differentially expressed genes. Furthermore, invasive carcinoma contained 2,756 ± 87 differentially expressed genes compared with control, showing a significantly lower correlation coefficient ($R = 0.74 \pm 0.02$) compared with those of other three stages ($P < 0.01$). A hierarchical clustering analysis showed that the normal epithelium, papilloma (dysplasia), and invasive carcinoma could be well classified, whereas the gene expression patterns between papilloma and dysplasia were indistinguishable (Fig. 4). To further confirm the integrity of our cDNA microrarray system, we first evaluated the expression levels of three genes, which are generally well known to be cancer related. The results revealed the expression levels of *cyclin D1* (Rat mRNA for *cyclin D1*) and *Mdm2* (mouse *Mdm2* gene) to be elevated in invasive carcinoma following by dysplasia (Fig. 5). *Cyclin D1* was also overexpressed in papilloma. The expression of *APC* (mouse adenomatous polyposis coli) was down-regulated in invasive carcinoma following by dysplasia. These results were well correlated to the previous reports (29–33). We then statistically searched the differentially expressed genes during ESCC progression. Human ESCC develops more frequently from dysplasia than papilloma. We thus analyzed the differentially expressed genes among the following three stages, normal epithelium, dysplasia, and invasive carcinoma. By means of the Fisher criterion (34), we selected 41 up-regulated genes and nine down-regulated genes associated with the process of esophageal carcinogenesis (Table 2*A* and *B*). The gene lists contained the genes encoding for proteases and plasminogen activator receptor and those associated with cell adhesion and cell growth. In addition, some cancer-related

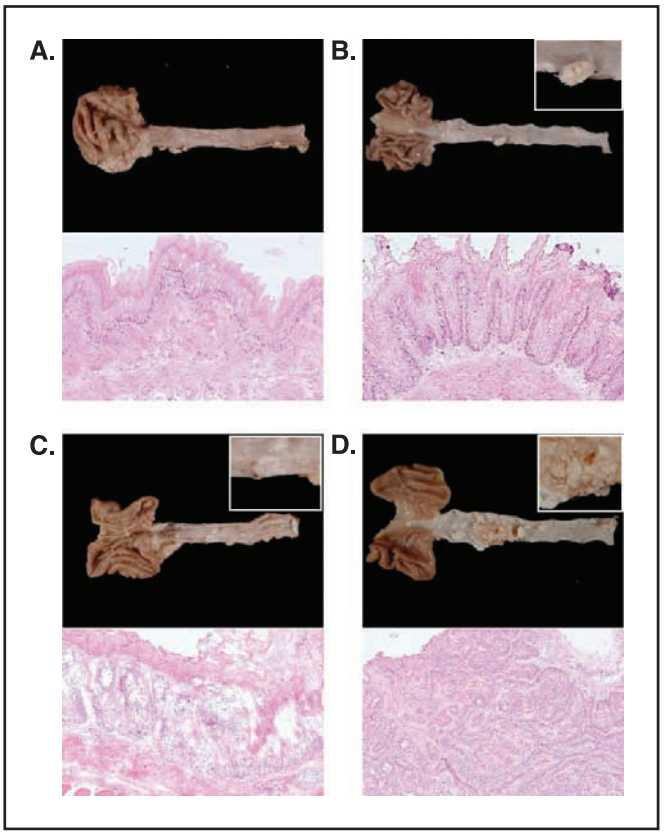

Figure 1. Macroscopic and microscopic findings (H&E staining) of each lesion of the rat esophagus. *A,* normal esophageal epithelium. *B,* papilloma. *C,* dysplasia. *D,* invasive carcinoma. In the microscopic findings, papilloma was characterized by squamous cell type exophytic tumors with hyperkeratinization and their basal layer was well preserved (*B*). Dysplasia included amorphous cells extending from the basal cell layer, except for a thin superficial layer (*C*). The invasion was beneath the basal layer and severe cellular atypism was present (*D*).

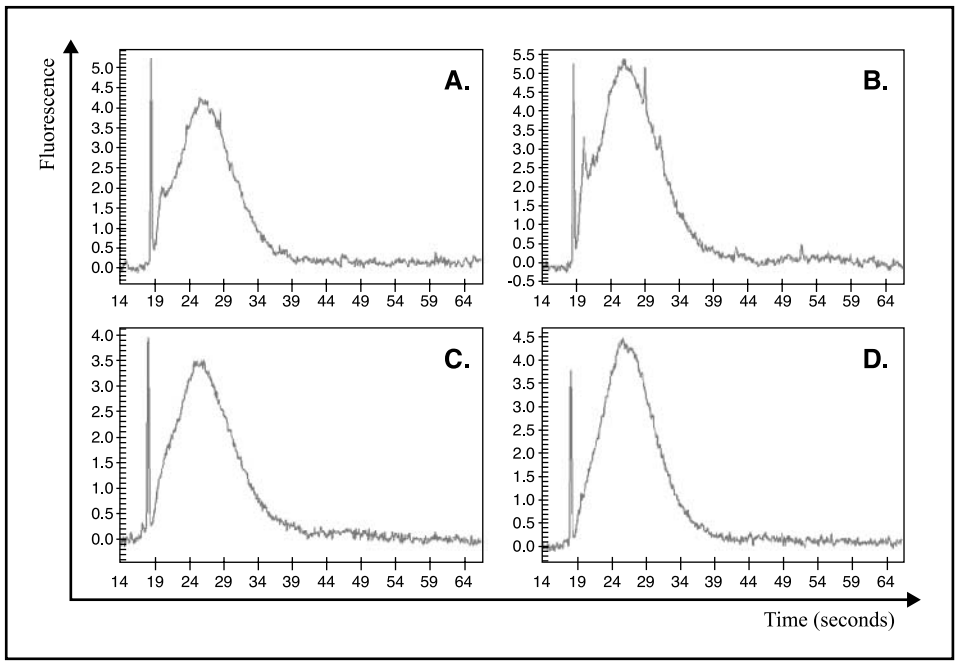

Figure 2. Representative electropherograms of successful RNA amplification from the normal epithelium (*A*), papilloma (*B*), dysplasia (*C*), and invasive carcinoma (*D*). They showed a hump peak and one marker peak. No contamination of the ribosomal RNA was detected.

genes, such as *Mmp2* (Rat matrix metalloproteinase 2 mRNA), *Ctsh* (Rat mRNA for cathepsin H), *Arhc* (Mouse rhoC mRNA), and *C1s* (Rat mRNA for serine protease) were also included.

Real-time RT-PCR Assay. In order to verify our cDNA microarray data, we did a real-time RT-PCR for some genes identified in Table 2*A* and *B*. The expression levels of real-time RT-PCR and the cDNA microarray are presented as the log ratio average of each three experiments (Fig. 6). These results corresponded very well to the microarray data for all six genes, thus strongly supporting the reliability and rationale of our strategy.

Discussion

To date, several studies have shown the gene expression patterns in human ESCC using DNA microarray technologies (7–13). Regarding animal models, the molecular mechanisms of carcinogenesis in the breast (14, 15), thyroid (16), liver (17), and stomach

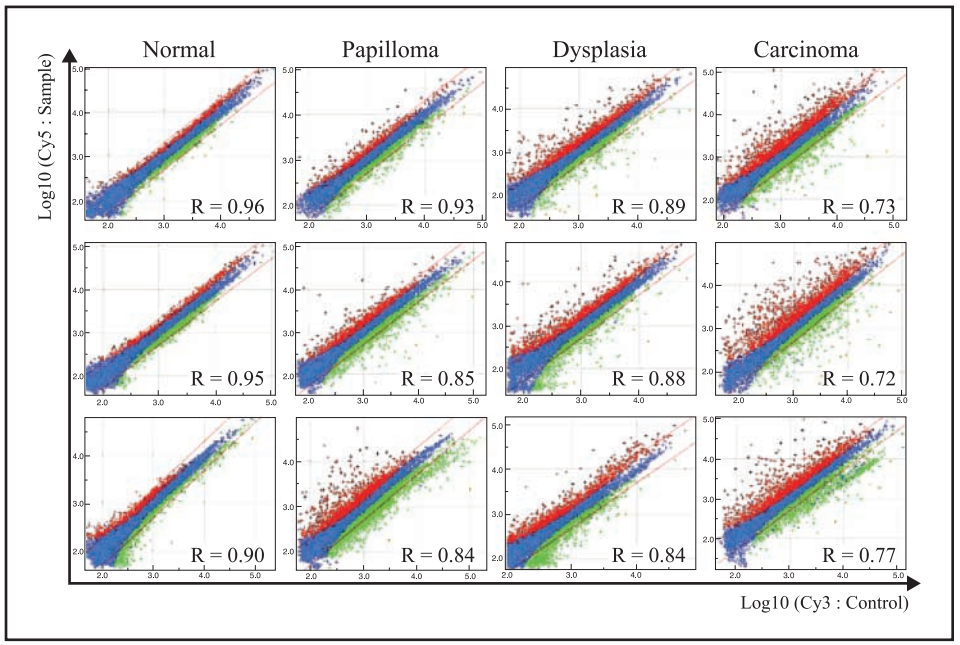

Figure 3. Intensity plots of a cDNA microarray in three samples each from normal epithelium, papilloma, dysplasia, and invasive carcinoma. *Red,* up-regulation into each sample; *green,* down-regulation; *blue,* unchanged based on the Rosetta Luminator error model ($P < 0.01$). The highest correlation coefficient ($R = 0.93 \pm 0.03$) was seen between the normal epithelium and control (mixture of three normal epithelium). The correlation coefficients in papilloma ($R = 0.87 \pm 0.05$) and dysplasia ($R = 0.87 \pm 0.03$) were intermediate. The gene expression profiles of invasive carcinoma and the control showed the lowest correlation coefficient ($R = 0.74 \pm 0.02$).

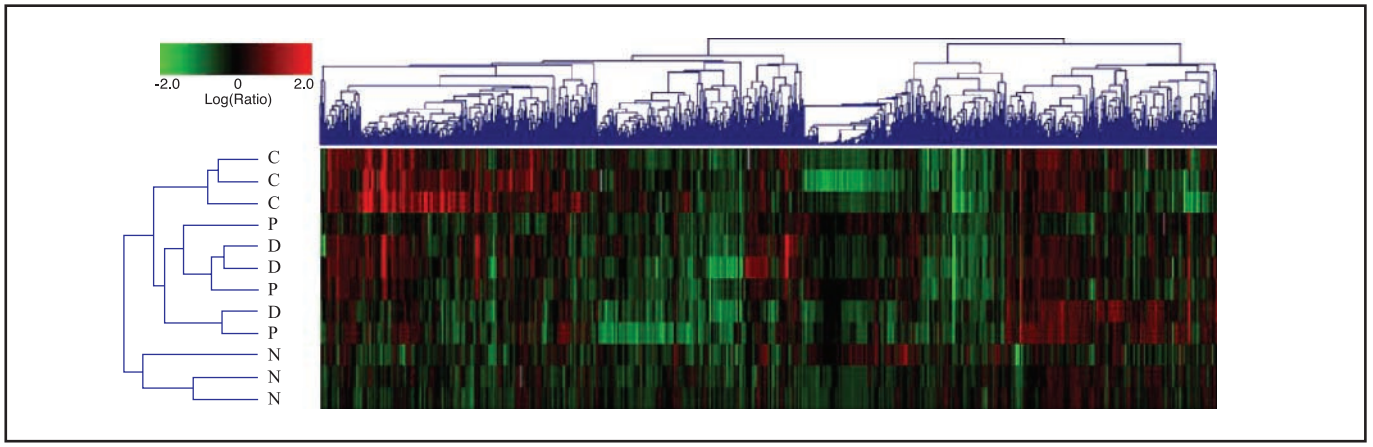

Figure 4. A hierarchical clustering analysis using 3,644 differentially expressed genes ($P < 0.01$). Three categories of normal epithelium, papilloma (dysplasia), and invasive carcinoma were well classified, whereas the expression patterns of papilloma and dysplasia were indistinguishable. *N,* normal epithelium; *P,* papilloma; *D,* dysplasia; *C,* invasive carcinoma.

(18) were evaluated using DNA microarrays, whereas no information is available for the gene expression profiles in an esophageal carcinogenesis model. The technical feasibility of a DNA microarray analysis for microdissected specimens in a rat liver carcinogenesis model has been recently reported (35). However, most of the previous studies examined the gene expression profiles in bulk tumor tissues, thus suggesting that these results might reflect heterogeneous expression profiles. In this study, we thus employed a technique of LMD to specifically isolate the cells from each esophageal lesion. The quality of RNA extracted from each specimen, which is extremely important for a DNA microarray analysis, was also carefully taken into account. We examined the quality of RNA using Agilent 2100 bioanalyzer, and we only used the specimens with high-quality RNA (Fig. 2). By combining the LMD and cDNA microarray, we showed that the number of differentially expressed genes markedly increased step-by-step from normal epithelium to dysplasia (papilloma) to invasive carcinoma (Fig. 3). It seems theoretically reasonable that the differences in the gene expression profiles between normal and

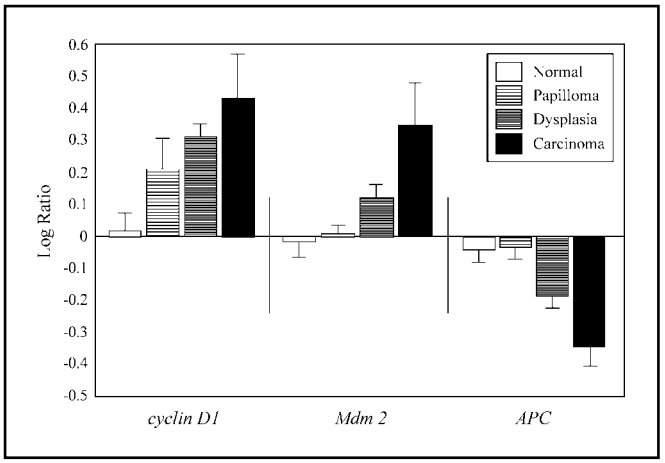

Figure 5. Results of a cDNA microarray for three genes, which are well known to be cancer-related genes. Expression levels of *cyclin D1* (Rat mRNA for *cyclin D1*) and *Mdm2* (Mouse *Mdm2* gene) were elevated in invasive carcinoma followed by dysplasia. Expression of *APC* (Mouse adenomatous polyposis coli) was markedly decreased in invasive carcinoma followed by dysplasia.

dysplasia (papilloma) was smaller than those between normal and invasive carcinoma. Lu et al. (7) have investigated gene expression profiles of five different stages during initiation and progression of human ESCC. They observed that the constant number of differentially expressed genes between the normal stage and stages of mild dysplasia (492 genes), moderate dysplasia (481 genes), carcinoma *in situ* (473 genes), and squamous cell carcinoma (501 genes). One possible explanation for the reason why, unlike us, they did not find a step-by-step increase in the number of differentially expressed genes might be attributable to differences in the species examined. Alternatively, we could reasonably show such a stepwise increase (Fig. 3), owing to the application of LMD to purify the cells from each lesion.

We observed the increased expression of *cyclin D1* not only in the dysplasia and carcinoma but also in the papilloma. A hierarchical clustering analysis did not distinguish the papilloma from dysplasia in our rat model. Furthermore, some previous reports have suggested that papilloma and hyperplastic lesions might be precancerous changes in rat esophageal carcinoma, as deduced from sequential morphologic studies (19, 36). On the other hand, human esophageal papilloma is a rare entity, which is not generally associated with the development of ESCC (37), whereas dysplasia has been well established as a precancerous lesion. These findings suggest that the association of rat papilloma with esophageal carcinogenesis may be different from that of human papilloma. The detailed differences remain to be determined.

The careful purification of cells from the normal epithelium, dysplasia, and invasive carcinoma, subsequent RNA isolation, and a cDNA microarray analysis identified 50 genes whose expression was associated with the development of rat ESCC (Table 2). For this step in the statistical analysis, we adopted the Fisher criterion because it takes variance into account unlike the Euclidean distance or the criterion based on a fold change. The up-regulated elements included the genes associated with cell adhesion (*Tmem8, Colla1, Lamc2,* and *Coll2a1*) and cell growth (*LynB* and *Arhc*). The genes coding for proteases (*Mmp2, Ctsh,* and *C1s*) were also up-regulated. Kan et al. (13) showed that the gene expression profiles of cancer tissues and those of cancer cell lines to be considerably different in human esophageal cancers using a cDNA microarray. One of the clearest distinctions was that the expression of proteases such as

Table 2. Genes associated with esophageal carcinogenesis

Accession no.	Symbol	Description	Gene ontology	Log ratio (average)		
				Normal	Dysplasia	Carcinoma
A. Forty-one up-regulated genes associated with the esophageal carcinogenesis						
U65656	*Mmp2**	Rat gelatinase A mRNA, complete cds. (matrix metalloproteinase 2)	metallopeptidase activity, carcinogenesis	−0.141	0.287	0.976
AB012026	*Krt2- 6a*	Mouse gene for keratin 6α, exon 2.	structural constituent of cytoskeleton	−0.117	1.194	1.637
X68273	*Cd68*	Mouse mRNA for macrosialin.	CD68 antigen, integral to membrane	−0.098	0.399	0.888
U32115	*Gp38*	Rat E11 antigen epitope (OTS- 8) mRNA, complete cds.	lung development	0.022	0.311	0.739
AB045293	*Tmem8*	Mouse mRNA for M83 protein, complete cds.	cell adhesion molecule activity	−0.231	0.444	0.964
AF000302	*LynB*	Rat Lyn B tyrosine kinase (LynB) mRNA, complete cds.	cell growth and/or maintenance	−0.038	0.263	0.760
U14914	*Ptprr*	Rat protein tyrosine phosphatase PC12- PTP1 (PTP) mRNA, complete cds.	transmembrane receptor activity	−0.525	0.121	0.606
D63774	*Krt14*	Rat mRNA for keratin 14, partial cds.	structural constituent of cytoskeleton	−0.103	0.297	0.932
X58861	*C1qa*	Mouse mRNA for complement subcomponent C1Q α- chain.	complement activity	−0.268	0.401	0.996
Y00708	*Ctsh**	Rat mRNA for cathepsin H (EC 3.4.22.16).	cysteine- type peptidase activity, carcinogenesis	−0.094	0.299	0.865
X71899	*Plaur*	Rat uPAR- 2 mRNA for urinary plasminogen activator receptor 2.	Plasminogen activator, urokinase receptor	−0.209	0.018	0.528
X56602	*G1p2*	Mouse mRNA Interferon- induced 15- kDa protein.	immune response	−0.243	0.056	0.692
AF004811	*Msn*	Rat moesin mRNA, complete cds.	structural molecule activity	0.052	0.470	0.897
Z78279	*Col1a1*	Rat mRNA for collagen α1 type I.	cell adhesion molecule activity	−0.169	0.047	0.961
AF165887	*Bcat1*	Rat cytosolic branch chain aminotransferase BCATc mRNA, partial cds.	transferase activity	−0.102	0.122	0.893
X15963	*Cox5a*	Mouse mRNA for cytochrome *c* oxidase subunit Va.	oxidoreductase activity	−0.039	0.148	0.772
AF176840	*Chst5*	Mouse intestine *N*- acetylglucosamine 6- *O*- sulfotransferase (I- GlcNAc- 6- ST) mRNA, complete cds.	transferase activity	−0.152	0.726	1.321
U43327	*Lamc2*	Mouse laminin γ2 chain (B2t) mRNA, complete cds.	cell adhesion molecule activity	0.020	0.329	0.740
D88250	*C1s**	Rat mRNA for serine protease, complete cds.	serine protease, carcinogenesis	0.082	0.606	1.139
U07201	*Asns*	Rat asparagine synthetase mRNA, secondary transcript, complete cds.	ligase activity	0.092	0.591	1.016
AF083269	*Arpc1b*	Rat p41- Arc mRNA, complete cds.	structural constituent of cytoskeleton, cell motility	0.110	0.439	0.826
U57362	*Col12a1*	Rat collagen XII α1 (Col12a1) mRNA, partial cds.	cell adhesion molecule activity	−0.041	0.131	0.992
AF010405	*Foxq1*	Mouse fork head transcription factor (Hfh- 1L) gene, complete cds.	transcription factor activity	0.114	0.369	0.766
AF135059	*Fbn1*	Rat fibrillin- 1 mRNA, complete cds.	cell adhesion molecule activity, metanephrogenesis	−0.036	0.281	0.914

(Continued on the following page)

Table 2. Genes associated with esophageal carcinogenesis (Cont'd)

Accession no.	Symbol	Description	Gene ontology	Log ratio (average)		
				Normal	Dysplasia	Carcinoma
M83143	*Siat1*	Rat β- galactoside- alpha 2,6- sialyltransferase mRNA.	transferase activity	−0.119	0.535	1.107
M38135	*Ctsh*	Rat cathepsin H (RCHII) mRNA.	cysteine- type peptidase activity, carcinogenesis	−0.003	0.387	0.947
AAF35394	*Gga2*	γ-adaptin related protein, GGA2	protein transporter activity	0.170	0.367	0.780
AF159593	*Plscr1*	Mouse phospholipid scramblase 1 mRNA, complete cds.	calcium ion binding	−0.120	0.260	0.957
X80638	*Arhc*	Mouse rhoC mRNA.	cell growth and/or maintenance, carcinogenesis	−0.002	0.153	0.784
U81829	*Calu*	Mouse calumenin mRNA, complete cds.	calcium ion binding protein	−0.241	−0.034	0.339
Z18877	*Oas1*	Rat mRNA for 2′ -5′ - oligoadenylate synthetase.	2'- 5'- oligoadenylate synthetase activity	−0.169	0.082	0.647
X51615	*Cx26*	Rat RNA for connexin protein Cx26.	gap junction membrane channel protein	0.031	0.306	1.000
BAA24267	*Farp1*	CDEP	Rho guanyl- nucleotide exchange factor activity	−0.277	0.032	0.624
AJ400844	*Pilra*	Mouse mRNA for imunoglobulin-like cell surface receptor FDF03.	protein binding	−0.339	−0.010	0.528
D86041	*Ddah1*	Rat mRNA for *N*-G,*N*-G-dimethylarginine dimethylaminohydrolase	hydrolase activity	−0.113	0.020	0.694
X70369	*Col3a1*	Rat mRNA for pro α1 collagen type III.	extracellular matrix structural constituent	−0.102	0.261	1.000
L03294	*Lpl*	Rat lipoprotein lipase mRNA, complete cds.	lipid transporter activity	−0.145	0.232	0.825
U06755	*Cnn3*	Rat Sprague- Dawley acidic calponin mRNA, complete cds.	actin bundling activity, calmodulin binding	0.018	0.272	0.930
J03026	*Mgp*	Rat matrix Gla protein mRNA, complete cds.	calcium ion binding	−0.138	0.442	1.446
AB008571	*Fhl2**	Rat mRNA for DRAL, complete cds.	protein binding	−0.088	0.273	0.905
L00193	*Krt1- 10*	Mouse epidermal keratin type I intermediate filament gene, exons 2 to 8.	structural constituent of cytoskeleton	0.111	0.943	1.354
B. Nine down-regulated genes associated with the esophageal carcinogenesis						
AF001896	*Aldh1a1**	Rat aldehyde dehydrogenase mRNA, complete cds.	oxidoreductase activity	0.022	−0.432	−0.911
BAA87047	*Mtvr2*	C184M protein	receptor activity	0.105	−0.297	−0.733
AF151982	*Slpi*	Rat secretory leukocyte protease inhibitor mRNA, complete cds.	inflammatory response regulate	0.032	−0.532	−1.150
AF121081	*Slc37a2*	Mouse cAMP inducible 2 protein (Ci2) mRNA, complete cds.	glycerol- 3- phosphate transporter activity	−0.109	−0.322	−0.918
AJ132356	*ArsB*	Mouse ARS component B gene, exons 1- 3.	cytokine activity	−0.108	−0.759	−1.427
AF017393	*Cyp2f1**	Rat cytochrome *P*4502F4 (CYP4502F4) mRNA, complete cds.	monooxygenase activity	−0.165	−0.508	−1.248
U04842	*Egf*	Rat preproepidermal growth factor mRNA, complete cds.	growth factor activity	0.121	−0.335	−0.757
CAA69194	*Pir*	Pirin	transcription cofactor activity	0.144	−0.198	−0.612
AAC17966	*Dscam*	Down syndrome cell adhesion molecule	cell adhesion molecule activity	0.066	−0.136	−0.667

*The gene expression levels were validated by real-time RT-PCR, and results are shown in Fig. 6.

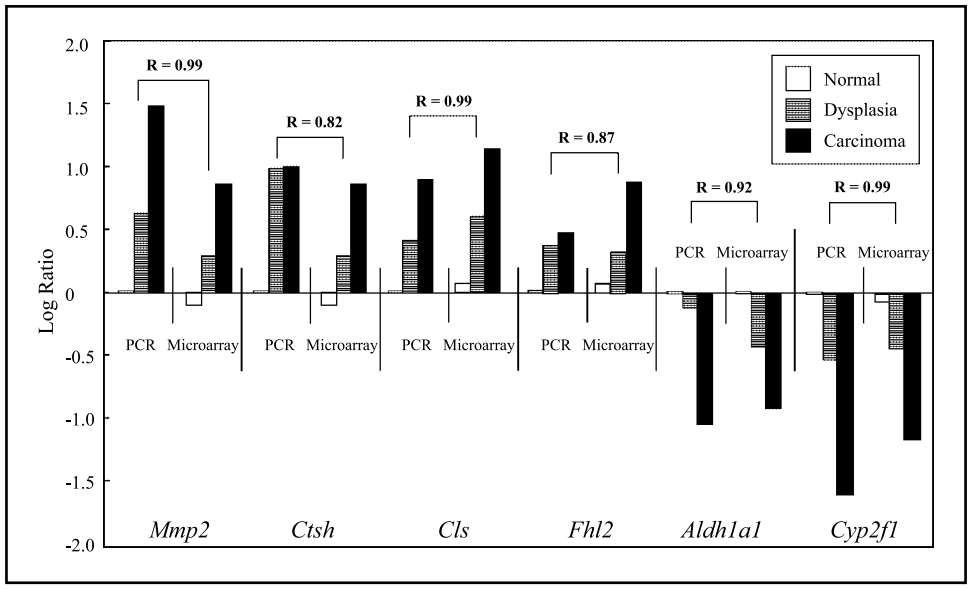

Figure 6. Validation of cDNA microarray data by real-time quantitative RT-PCR. Expression levels of the selected six genes using real-time RT-PCR corresponded very well to those using a cDNA microarray for the normal epithelium, dysplasia, and invasive carcinoma (R = 0.82-0.99). Results verify the reliability of our cDNA microarray experiments.

matrix metalloproteinases and plasminogen activators was high in most cancer tissues, whereas it was low in the cancer cell lines. In the present study, we found the stepwise increases of proteases including matrix metalloproteinase 2 (*Mmp2*), Cathepsin H (*Ctsh*), a serine protease (*C1s*) as shown in Fig. 6. The expression of *Mmp2* has been found to be correlated with cancer cell migration and invasion (38, 39). Recently, these proteases have gotten a lot of attention as a therapeutic target for invasive carcinomas (40). A lysosomal cysteine protease, *Ctsh* plays a central role in the cellular processes such as the degradation of intracellular proteins, extracellular matrix remodeling, and apoptosis (41). The overexpression of *Ctsh* has been associated with the malignant progression of a variety of cancers (42, 43). The family of enzymes, known as serine protease (*C1s*), supports many biological functions for cancer cells, including the activation of growth and angiogenic factors and the activation of other proteases for invasion and metastasis. Several genes encoding enzymes associated with cell adhesion and degradation, including urinary plasminogen activator receptor 2 (*Plaur*) also increased (Table 2*A*). In addition, a protease inhibitor (*Slpi*) showed stepwise a decrease from the normal epithelium to dysplasia to invasive carcinoma. These findings support the importance of examining the gene expression profiles of "*in vivo*" cancer cells isolated by a LMD and may also suggest the limitation of "*in vitro*" studies of cancer cell lines. This genome-wide global information obtained herein will hopefully contribute to an improved understanding of the molecular alterations that occur during the development of ESCC, and also potentially help to establish novel diagnostic and therapeutic targets. Because the present study proves the usefulness of this approach, other studies are presently under way to obtain additional information on these molecular pathways using esophageal specimens from patients with ESCC.

Acknowledgments

Received 8/9/2004; revised 10/16/2004; accepted 11/10/2004.

Grant support: Long-range Research Initiative project of the Japan Chemical Industry Association; Japan Society for the Promotion of Science Grant-in-Aid for Scientific Research 15390398; Ministry of Education, Culture, Sports, Science, and Technology of Japan Grant-in-Aid for Scientific Research on Priority Areas 15023245; and a Health and Labor Sciences Research Grant on Hepatitis and BSE 14230801, Ministry of Health, Labor, and Welfare of Japan.

The costs of publication of this article were defrayed in part by the payment of page charges. This article must therefore be hereby marked advertisement in accordance with 18 U.S.C. Section 1734 solely to indicate this fact.

We thank Haruko Yasunami, Mayumi Oda, Mayumi Ikeda, and Kazue Ogata for their excellent technical assistance.

References

1. Matsufuji H, Ueo H, Mori M, Kuwano H, Sugimachi K. Enhancement of esophageal carcinogenesis induced in rats by *N*-amyl-*N*-methylnitrosamine in the presence of 12-*O*-tetradecanoylphorbol-13-acetate. J Natl Cancer Inst 1987;79:1123–9.
2. Vogelstein B, Fearon ER, Hamilton SR, et al. Genetic alterations during colorectal-tumor development. N Engl J Med 1988;319:525–32.
3. Cho KR, Vogelstein B. Genetic alterations in the adenoma–carcinoma sequence. Cancer 1992;70:1727–3.
4. Shinozaki H, Ozawa S, Ando N, et al. Cyclin D1 amplification as a new predictive classification for squamous cell carcinoma of the esophagus, adding gene information. Clin Cancer Res 1996;2:1155–61.
5. Opitz OG, Harada H, Suliman Y, et al. A mouse model of human oral-esophageal cancer. J Clin Invest 2002;110:761–9.
6. Wang LD, Hong JY, Qiu SL, Gao H, Yang CS. Accumulation of p53 protein in human esophageal precancerous lesions: a possible early biomarker for carcinogenesis. Cancer Res 1993;53:1783–7.
7. Lu J, Liu Z, Xiong M, et al. Gene expression profile changes in initiation and progression of squamous cell carcinoma of esophagus. Int J Cancer 2001;91:288–94.
8. Kihara C, Tsunoda T, Tanaka T, et al. Prediction of sensitivity of esophageal tumors to adjuvant chemotherapy by cDNA microarray analysis of gene-expression profiles. Cancer Res 2001;61:6474–9.
9. Su LK, Kinzler KW, Vogelstein B, et al. Multiple intestinal neoplasia caused by a mutation in the murine homolog of the APC gene. Science 1992;256:668–70.
10. Luo A, Kong J, Hu G, et al. Discovery of Ca2+-relevant and differentiation-associated genes downregulated in esophageal squamous cell carcinoma using cDNA microarray. Oncogene 2004;23:1291–9.
11. Hu YC, Lam KY, Law S, Wong J, Srivastava G. Profiling of differentially expressed cancer-related genes in esophageal squamous cell carcinoma (ESCC) using human cancer cDNA arrays: overexpression of oncogene MET correlates with tumor differentiation in ESCC. Clin Cancer Res 2001;7:3519–25.

12. Hu YC, Lam KY, Law S, Wong J, Srivastava G. Identification of differentially expressed genes in esophageal squamous cell carcinoma (ESCC) by cDNA expression array: overexpression of Fra-1, Neogenin, Id-1, and CDC25B genes in ESCC. Clin Cancer Res 2001;7:2213–21.

13. Kan T, Shimada Y, Sato F, et al. Gene expression profiling in human esophageal cancers using cDNA microarray. Biochem Biophys Res Commun 2001;286: 792–801.

14. Wang Y, Hu L, Yao R, et al. Altered gene expression profile in chemically induced rat mammary adenocarcinomas and its modulation by an aromatase inhibitor. Oncogene 2001;20:7710–21.

15. Kuramoto T, Morimura K, Yamashita S, et al. Etiology-specific gene expression profiles in rat mammary carcinomas. Cancer Res 2002;62:3592–7.

16. Ying H, Suzuki H, Furumoto H, et al. Alterations in genomic profiles during tumor progression in a mouse model of follicular thyroid carcinoma. Carcinogenesis 2003;24:1467–79.

17. Tellgren A, Wood TJ, Flores-Morales A, Torndal UB, Eriksson L, Norstedt G. Differentially expressed transcripts in neoplastic hepatic nodules and neonatal rat liver studied by cDNA microarray analysis. Int J Cancer 2003;104:131–8.

18. Abe M, Yamashita S, Kuramoto T, et al. Global expression analysis of *N*-methyl-*N*′-nitro-*N*-nitrosoguanidine-induced rat stomach carcinomas using oligonucleotide microarrays. Carcinogenesis 2003;24:861–7.

19. Sasajima K, Taniguchi Y, Okazak S, et al. Sequential morphological studies of the esophageal carcinoma of rats induced by *N*-methyl-*N*-amylnitrosamine. Eur J Cancer Clin Oncol 1982;18:559–64.

20. Iizuka T, Ichimura S, Kawachi T. Esophageal carcinoma in rats induced by *N*-amyl-*N*-methylnitrosamine. Gann 1980;71:94–9.

21. Reuber MD. Histopathology of preneoplastic and neoplastic lesions of the esophagus in BUF rats ingesting diethylnitrosamine. J Natl Cancer Inst 1977;58:313–21.

22. Mori M, Mimori K, Yoshikawa Y, et al. Analysis of the gene-expression profile regarding the progression of human gastric carcinoma. Surgery 2002;131:S39–47.

23. Van Gelder RN, von Zastrow ME, Yool A, Dement WC, Barchas JD, Eberwine JH. Amplified RNA synthesized from limited quantities of heterogeneous cDNA. Proc Natl Acad Sci U S A 1990;87:1663–7.

24. Eberwine J, Yeh H, Miyashiro K, et al. Analysis of gene expression in single live neurons. Proc Natl Acad Sci U S A 1992;89:3010–4.

25. Utsunomiya T, Okamoto M, Hashimoto M, et al. A gene-expression signature can quantify the degree of rat hepatic fibrosis. J Hepatol 2004;41:399–406.

26. Yang YH, Dudoit S, Luu P, et al. Normalization for cDNA microarray data: a robust composite method addressing single and multiple slide systematic variation. Nucleic Acids Res 2002;30:e15.

27. Luo L, Salunga RC, Guo H, et al. Gene expression profiles of laser-captured adjacent neuronal subtypes. Nat Med 1999;5:117–22.

28. Okabe H, Satoh S, Kato T, et al. Genome-wide analysis of gene expression in human hepatocellular carcinomas using cDNA microarray: identification of genes involved in viral carcinogenesis and tumor progression. Cancer Res 2001;61:2129–37.

29. Zhang T, Nanney LB, Luongo C, et al. Concurrent overexpression of cyclin D1 and cyclin-dependent kinase 4 (Cdk4) in intestinal adenomas from multiple intestinal neoplasia (Min) mice and human familial adenomatous polyposis patients. Cancer Res 1997;57: 169–75.

30. Jenkins TD, Mueller A, Odze R, et al. Cyclin D1 overexpression combined with *N*-nitrosomethylbenzylamine increases dysplasia and cellular proliferation in murine esophageal squamous epithelium. Oncogene 1999;18:59–66.

31. Jones SN, Hancock AR, Vogel H, Donehower LA, Bradley A. Overexpression of Mdm2 in mice reveals a p53-independent role for Mdm2 in tumorigenesis. Proc Natl Acad Sci U S A 1998;95:15608–12.

32. Ganguli G, Abecassis J, Wasylyk B. MDM2 induces hyperplasia and premalignant lesions when expressed in the basal layer of the epidermis. EMBO J 2000; 19:5135–47.

33. Morin PJ, Vogelstein B, Kinzler KW. Apoptosis and APC in colorectal tumorigenesis. Proc Natl Acad Sci U S A 1996;93:7950–4.

34. Iizuka N, Oka M, Yamada-Okabe H, et al. Oligonucleotide microarray for prediction of early intrahepatic recurrence of hepatocellular carcinoma after curative resection. Lancet 2003;361:923–9.

35. Michel C, Desdouets C, Sacre-Salem B, Gautier JC, Roberts R, Boitier E. Liver gene expression profiles of rats treated with clofibric acid: comparison of whole liver and laser capture microdissected liver. Am J Pathol 2003;163:2191–9.

36. Napalkov NP, Pozharisski KM. Morphogenesis of experimental tumors of the esophagus. J Natl Cancer Inst 1969;42:927–40.

37. Talamini G, Capelli P, Zamboni G, et al. Alcohol, smoking and papillomavirus infection as risk factors for esophageal squamous-cell papilloma and esophageal squamous-cell carcinoma in Italy. Int J Cancer 2000;86:874–8.

38. Davies B, Waxman J, Wasan H, et al. Levels of matrix metalloproteases in bladder cancer correlate with tumor grade and invasion. Cancer Res 1993; 53:5365–9.

39. Mori M, Mimori K, Shiraishi T, et al. Analysis of MT1-MMP and MMP2 expression in human gastric cancers. Int J Cancer 1997;74:316–21.

40. Ueda J, Kajita M, Suenaga N, Fujii K, Seiki M. Sequence-specific silencing of MT1-MMP expression suppresses tumor cell migration and invasion: importance of MT1-MMP as a therapeutic target for invasive tumors. Oncogene 2003;22:8716–22.

41. Chapman HA, Riese RJ, Shi GP. Emerging roles for cysteine proteases in human biology. Annu Rev Physiol 1997;59:63–88.

42. del Re EC, Shuja S, Cai J, Murnane MJ. Alterations in cathepsin H activity and protein patterns in human colorectal carcinomas. Br J Cancer 2000;82: 1317–26.

43. Waghray A, Keppler D, Sloane BF, Schuger L, Chen YQ. Analysis of a truncated form of cathepsin H in human prostate tumor cells. J Biol Chem 2002;277: 11533–8.

Global Analysis of Altered Gene Expressions during the Process of Esophageal Squamous Cell Carcinogenesis in the Rat: A Study Combined with a Laser Microdissection and a cDNA Microarray

Koujiro Nishida, Shinji Mine, Tohru Utsunomiya, et al.

Cancer Res 2005;65:401-409.